J|A|C|S
ARTICLES

Published on Web 12/08/2010

Self-Accumulation of Aromatics at the Oil−Water Interface through Weak Hydrogen Bonding

Makoto Kunieda,[†] Kennichi Nakaoka,[†] Yunfeng Liang,*[,†] Caetano R. Miranda,[†,‡] Akira Ueda,[†] Satoru Takahashi,[§] Hiroshi Okabe,[§] and Toshifumi Matsuoka*[,†]

Department of Urban Management, Kyoto University, Kyoto 615-8540, Japan, Universidade Federal do ABC, Rua Santa Adélia, 166 Bangu 09210-170, Santo André, SP Brazil, and Japan Oil, Gas and Metals National Corporation, Chiba 261-0025, Japan

Received August 22, 2010; E-mail: y_liang@earth.kumst.kyoto-u.ac.jp; matsuoka@earth.kumst.kyoto-u.ac.jp

Abstract: It is well-known that the amphiphilic solutes are surface-active and can accumulate at the oil−water interface. Here, we have investigated the water and a light-oil model interface by using molecular dynamic simulations. It was found that aromatics concentrated in the interfacial region, whereas the other hydrocarbons were uniformly distributed throughout the oil phase. Similar to previous studies, such concentrations were not observed at pure aromatics−water interfaces. We show that the self-accumulation of aromatics at the oil−water interface is driven by differences in the interfacial tension, which is lower for aromatics−water than between the others. The weak hydrogen bonding between the aromatic rings and the water protons provides the mechanism for lowering the interfacial tension.

Downloaded via LOUISIANA STATE UNIV on April 2, 2023 at 19:59:56 (UTC).
See https://pubs.acs.org/sharingguidelines for options on how to legitimately share published articles.

Introduction

The interfaces between two immiscible liquids are ubiquitous and play an important role in many natural and technological processes.[1−5] Unlike the bulk materials, the interface system is a noncentrosymmetric environment about which we know very little. Experimental measurements for liquid−liquid interfaces are challenging[6−11] because of the relatively small size—typically only a few molecular diameters wide—and the buried nature of the interface. Enhanced oil recovery (EOR) techniques to increase the crude oil production from oil reservoirs are increasingly important for the energy security, as the reserves are limited. There are many EOR techniques including gas injection and chemical injection, among others.[12] The main approach to EOR is to decrease the interfacial tension (IFT) or the viscosity of the crude oil through molecular additives that are adsorbed at the oil−water interface or migrate into the crude oil through the interface. It is important, therefore, for the phenomena pertaining to the crude oil and underground fluid (usually aqueous) interface to be understood.

In the past, much experimental work has been carried out to understand the properties of water next to hydrophobic surfaces,[7,8] including the orientation of water and its hydrogen bonding. However, there has been little exploration of the structural properties of oil next to the interface. Although computational approaches such as molecular dynamics and Monte Carlo simulations can provide insights into the structural properties of oil−water interfacial systems,[13−18] most studies have been limited to the stable interfacial structure of a pure hydrocarbon−water system[13−17] or that with surfactant.[18] However, crude oil is a highly complex material[12] that consists mainly of hydrocarbons but can hardly be described as a single hydrocarbon phase. In particular, it is widely accepted that the percentage contents of paraffinic (alkane), naphthenic (cycloalkane), and aromatic components in reservoir fluids (often referred to as the PNA distribution) are essential properties when describing crude oil.[12] Recent experimental studies have reported that trace impurities can significantly modify the interfacial tension, by up to 10−20 mN/m, over a period of a few hours.[6] Theoretical investigations have also shown that even mixtures containing

[†] Kyoto University.
[‡] Universidade Federal do ABC.
[§] Japan Oil, Gas and Metals National Corporation.

(1) Benjamin, I. *Annu. Rev. Phys. Chem.* **1997**, *48*, 407–451.
(2) Jungwirth, P.; Finlayson-Pitts, B. J.; Tobias, D. J. *Chem. Rev.* **2006**, *106*, 1137–1139.
(3) Chandler, D. *Nature* **2007**, *445*, 831–832.
(4) Hore, D. K.; Walker, D. S.; Richmond, G. L. *J. Am. Chem. Soc.* **2008**, *130*, 1800–1801.
(5) Bonn, D.; Eggers, J.; Indekeu, J.; Meunier, J.; Rolley, E. *Rev. Mod. Phys.* **2009**, *81*, 739–805.
(6) Mitrinovic, D. M.; Tikhonov, A. M.; Li, M.; Huang, Z.; Schlossman, M. L. *Phys. Rev. Lett.* **2000**, *85*, 582–585.
(7) Du, Q.; Freysz, E.; Shen, Y. R. *Science* **1994**, *264*, 826–828.
(8) Scatena, L. F.; Brown, M. G.; Richmond, G. L. *Science* **2001**, *292*, 908–912.
(9) De Serio, M.; Mohapatra, H.; Zenobi, R.; Deckert, V. *Chem. Phys. Lett.* **2006**, *417*, 452–456.
(10) Nomoto, T.; Onishi, H. *Phys. Chem. Chem. Phys.* **2007**, *9*, 5515–5521.
(11) Lambert, J.; Hergenröder, R.; Suter, D.; Deckert, V. *Angew. Chem., Int. Ed.* **2009**, *48*, 6343–6345.
(12) Petersen, K. S.; Christensen, P. L. *Phase Behavior of Petroleum Reservoir Fluids*; CRC Press: Boca Raton, London and New York, 2007.
(13) Linse, P. *J. Chem. Phys.* **1987**, *86*, 4177–4187.
(14) Kereszturi, I.; Jedlovszky, P. *J. Phys. Chem. B* **2005**, *109*, 16782–16793.
(15) van Buuren, A.; Marrink, S.; Berendsen, H. *J. Phys. Chem.* **1993**, *97*, 9206–9212.
(16) Bresme, F.; Chacon, E.; Tarazona, P.; Tay, K. *Phys. Rev. Lett.* **2008**, *101*, 056102.
(17) Patel, S. A.; Brooks, C. L. *J. Chem. Phys.* **2006**, *124*, 204706.
(18) Jang, S. S.; Lin, S.-T.; Maiti, P. K.; Blanco, M.; Goddard, W. A., III; Shuler, P.; Tang, Y. J. *Phys. Chem. B* **2004**, *108*, 12130–12140.

 © 2010 American Chemical Society

only *n*-alkanes exhibit exotic phenomena compared with a single-component system.[19] Here, we present a more realistic light-oil model. The purpose of this work was to study the molecular organization and the interfacial properties of a complex oil−water system and to compare these results with those of pure hydrocarbon−water systems. Three types of system were used for the interfacial simulations: a light-oil model−water system, pure hydrocarbon−water systems, and a hep−tol (1:1 mixture of heptane and toluene, by volume)−water system. In previous studies, a small number of hydrocarbons were typically employed to investigate the oil−water interfaces, which resulted in low statistical accuracy regarding the structural properties (e.g., insufficient resolution on the density profile), thereby obscuring the structural features.[13−15] To overcome this difficulty, large-scale molecular dynamic simulations were engaged in this work. A typical interface system contained approximately 1000 hydrocarbon molecules and 7000−8000 H_2O molecules, giving a total of about 50 000 atoms.

Computational Methods

The light-oil model we used in this study was a mixture of eight hydrocarbons: hexane, heptane, octane, nonane, cyclohexane, cycloheptane, benzene, and toluene, with 144, 132, 156, 180, 96, 156, 60, and 156 molecules, respectively. The composition has high relevance to light crude oil in Japanese oil fields and is typical for modeling gasoline. Molecular dynamics (MD) simulations were performed using the GROMACS package.[20] The water molecules were modeled by SPC/E (single point charge/extended),[21,22] as it can reproduce the surface tension of water and orthobaric densities as well as other structural properties of liquid water.[22] A revised version of the CHARMM27 force field[23] was used to model the hydrocarbons, except for benzene, where different charges were used (see below for an explanation). The pure hydrocarbons and the water were calculated from isobaric−isothermal ensemble (NPT) simulation, whereas the interface systems were performed in the isobaric−isothermal−isointerface area ensemble (NPnAT). In all calculations, the temperature was controlled by the Nose−Hoover thermostat,[24] and the pressure was controlled by the Parrinello−Rahman method.[25] The particle mesh Ewald summation[26] was used for the electrostatic interactions, and a cutoff of 14 Å was used for the van der Waals interactions. A 1.0 fs time step was used and the coordinates output every 1.0 ps. The accuracies of each hydrocarbon model were confirmed by comparison with experimental properties. The equilibrium densities of these pure hydrocarbons from NPT simulation at ambient condition were in excellent agreement with experimental values (Table 1).[27] More importantly, the hierarchy of the densities of the *n*-alkanes, cycloalkanes, and aromatics was well-reproduced. The IFTs between the hydrocarbons and the SPC/E water are presented in the Table 1. These values also agree with experimental data.[28−32] The IFTs of *n*-alkanes and cycloalkanes with the SPC/E water are around 50 mN/m, whereas those of aromatics with SPC/E water are around 35 mN/m, 15 mN/m lower than those of *n*-alkanes and cycloalkanes. Therefore, each hydrocarbon model reasonably served as a component in the light-oil model.

Table 1. Densities of Pure Hydrocarbons and Interfacial Tensions of Hydrocarbon−Water Interface Systems at 298 K and 0.1 MPa, in Comparison with Available Experimental Data (Refs 27−32)

	density (kg/m^3)		interfacial tension with SPC/E water (mN/m)	
system	MD	experiment[a]	MD	experiment
n-hexane	654.27	654.92	50.73	50.5[b], 51.4[c], 49.7[d]
n-heptane	679.64	679.72	51.96	51.9[c], 50.2[d]
n-octane	699.12	698.39	52.72	50.7[b], 52.5[c], 50.2[d]
n-nonane	715.70	714.21	52.77	50.9[b], 52.4[c]
cyclohexane	754.02	774.03	49.53	49.6[b], 50.0[d]
cycloheptane	791.37	811.00	53.48	
benzene	874.74	873.83	34.42	34.4[b], 35.8[e], 33.7[f], 34.7[d]
toluene	867.45	862.38	37.69	36.0[e], 36.4[f], 36.1[d]

[a] Ref 27. [b] Ref 28. [c] Ref 30. [d] Ref 32. [e] Ref 29. [f] Ref 31.

Results and Discussion

Light-Oil Model and Water Interface: Self-Accumulation of the Aromatics. We studied the interface between the light-oil model and water. A typical snapshot of a unit cell for the MD calculation of the interface system under 298 K and 0.1 MPa is shown in Figure 1a. The density profiles across the water and light-oil model system interface after NPnAT equilibration at 298 K and 0.1 MPa and at 400 K and 30 MPa are illustrated in Figure 1, parts b and c, respectively. The accumulation of aromatics (benzene and toluene) at the interface of water and the light-oil model was observed at all the thermal conditions we studied. The interface system was divided into three regions: the water region, the interface region (that is, the aromatics-rich region), and the bulk oil region. At 298 K and 0.1 MPa, the maximum density of aromatics in the interface region is 3.5−4.0 times higher than their densities in the bulk oil region (see the inset of Figure 1b). This value approaches 1.8 at a typical reservoir condition of 400 K and 30 MPa. The calculated IFT of the light-oil−water system at 298 K and 0.1 MPa is 47.49 mN/m or ∼5 mN/m lower than that of a typical *n*-alkane−water interfacial system. It is noteworthy that such an aromatic concentration is not observed at pure hydrocarbon−water interfaces, including benzene−water and toluene−water (Figure 2a). In summary, the aromatics (though not amphiphilic) are "surface-active" at the oil−water interface but are "inactive" at the pure aromatics−water interface. This is the main finding of this work. We hypothesize that the accumulation is driven by the inherent interfacial tension difference between aromatics−water and the other potential hydrocarbons−water interface combinations. When aromatic molecules accumulate at the interface, the configuration entropy, *S*, decreases, similar to the case for the adsorption of surfactants and alkanols,[33] and the Gibbs free energy increases within the interface system. On the other hand, the IFTs of the aromatics are 10−15 mN/m lower than those of *n*-alkanes and cycloalkanes (Table 1) so the accumulation of aromatics causes a decrease in interfacial

(19) Xia, T. K.; Landman, U. *Science* **1993**, *261*, 1310–1312.
(20) Hess, B.; Kutzner, C.; van der Spoel, D.; Lindahl, E. *J. Chem. Theory Comput.* **2008**, *4*, 435–447.
(21) Berendsen, H.; Grigera, J.; Straatsma, T. *J. Phys. Chem.* **1987**, *91*, 6269–6271.
(22) Alejandre, J.; Tildesley, D.; Chapela, G. *J. Chem. Phys.* **1995**, *102*, 4574–4583.
(23) Klauda, J.; Brooks, B.; MacKerell, A., Jr.; Venable, R.; Pastor, R. J. *Phys. Chem. B* **2005**, *109*, 5300–5311.
(24) Nose, S. *Mol. Phys.* **1984**, *52*, 255–268.
(25) Parrinello, M.; Rahman, A. *J. Chem. Phys.* **1982**, *76*, 2662–2666.
(26) Essmann, U.; Perera, L.; Berkowitz, M. L.; Darden, T.; Lee, H.; Pedersen, L. G. *J. Chem. Phys.* **1995**, *103*, 8577–8593.
(27) Lemmon, E. W.; McLinden, M. O.; Friend, D. G. *Thermophysical Properties of Fluid Systems, NIST Chemistry WebBook, NIST Standard Reference Database No. 69*; Linstrom, P. J., Mallard, W. G., Eds.; National Institutes of Standards and Technology: Gaithersburg, MD, 2005.
(28) Rehfeld, S. *J. Phys. Chem.* **1967**, *71*, 738–745.
(29) Yeung, A.; Dabros, T.; Masliyah, J. J. *Colloid Interface Sci.* **1998**, *208*, 241–247.
(30) Goebel, A.; Lunkenheimer, K. *Langmuir* **1997**, *13*, 369–372.
(31) Moran, K.; Yeung, A.; Masliyah, J. *Langmuir* **1999**, *15*, 8497–8504.
(32) Donahue, D.; Bartell, F. *J. Phys. Chem.* **1952**, *56*, 480–489.
(33) Takiue, T.; Uemura, A.; Ikeda, N.; Motomura, K.; Artono, M. *J. Phys. Chem. B* **1998**, *102*, 3724–3729.

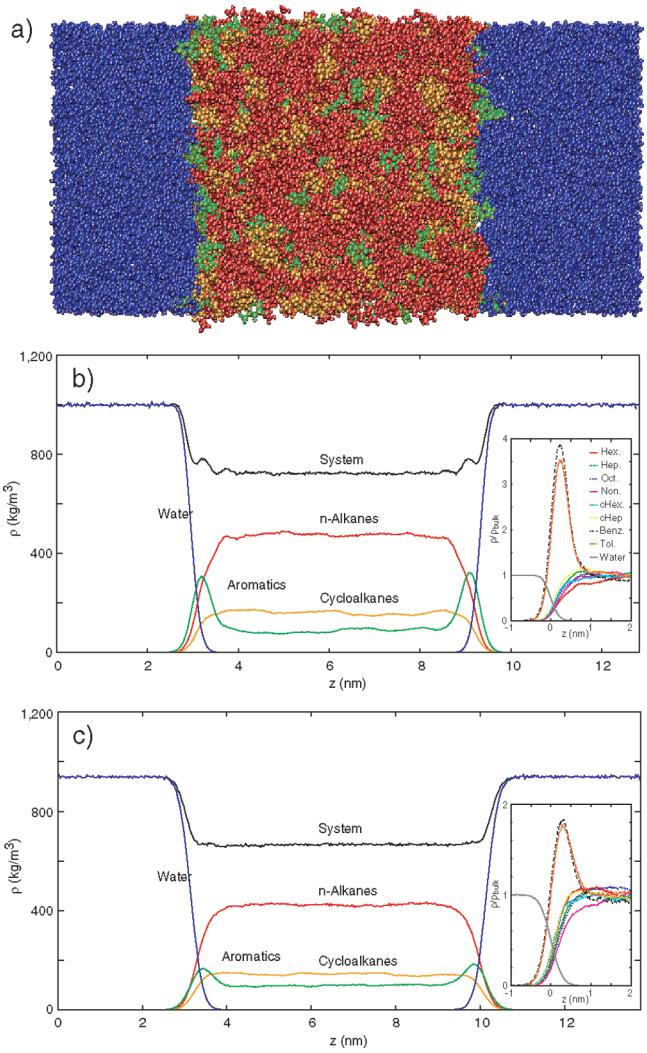

Figure 1. (a) Snapshot of the light-oil model−water interface system at 298 K and 0.1 MPa taken after 5.0 ns of NPnAT simulation (red, *n*-alkanes; orange, cycloalkanes; green, aromatics; blue, water). (b) The density profiles of the total interfacial system, *n*-alkanes, cycloalkanes, aromatics, and water, along the *z*-axis averaged over 3.0−5.0 ns at 298 K and 0.1 MPa and (c) at 400 K and 30 MPa. Insets: the normalized "individual" density profile, namely, $\rho(z)/\rho_{bulk}$, which averages on the basis of two quasi-symmetric interfaces.

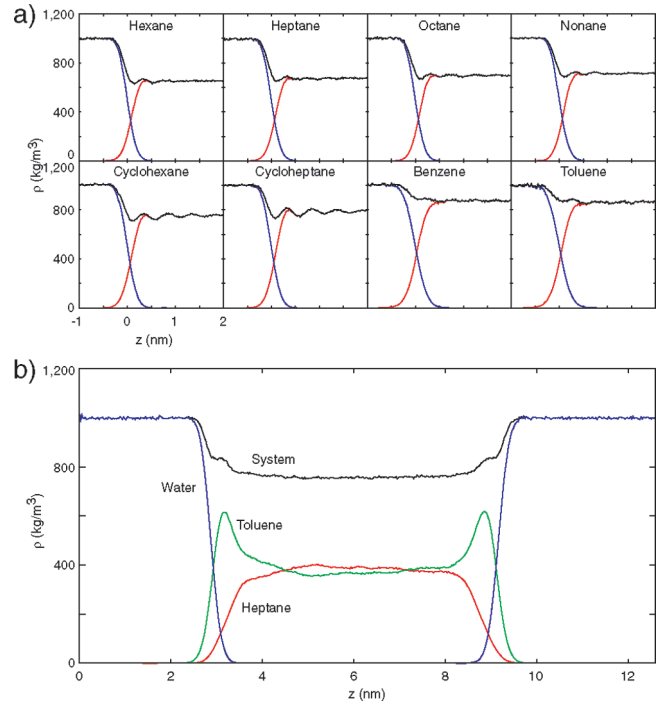

Figure 2. (a) Averaged density profiles of the interface systems for pure hydrocarbon−water interfacial systems along the *z*-axis at 298 K and 0.1 MPa for 1.5−2.0 ns (black, system; red, hydrocarbon; blue, water) and (b) heptane−toluene−water system for 3.0−5.0 ns. Note the very different density profile (i.e., a sharp density peak) of toluene inside the heptane−toluene mixture−water interface and the one (i.e., no density peak) inside the pure toluene−water interface. All pure hydrocarbon−water interfaces present a clear interface. A longer simulation (∼5 ns) is required for the mixture−water interface (e.g., heptane−toluene−water interface) than the pure hydrocarbon−water interface system (∼2 ns) to obtain a converged interfacial tension.

tension, γ, therefore decreasing the potential energy of the total system. Consequently, the Gibbs free energy reaches a minimum value with the accumulation of aromatics at equilibrium.

Hep−Tol−Water Interface: Interfacial Tension Difference Is the Driving Force of the Accumulation. To corroborate our hypothesis, a hep−tol−water system was prepared in an ad hoc manner. Figure 2b shows the density profiles for the hep−tol−water system after NPnAT equilibration. As anticipated, the accumulation of toluene at the hep−tol−water interfaces was observed. Similar to the light-oil−water system, the density profiles can be divided into three regions: the water region, the interface region (i.e., the toluene-rich region), and the bulk hep−tol region. The density of the bulk hep−tol region (4 nm $< z <$ 8 nm) was 760 kg/m^3, which is slightly lower than that of the pure hep−tol system (773.19 kg/m^3). This occurs simply because the amount of toluene in the bulk hep−tol region is reduced due to the accumulation of toluene at the interface so that the hep−tol region is no longer a 1:1 mixture, by volume, of heptane and toluene. The maximum concentration of toluene at the interface region is nearly 1.6 times larger than that in the bulk hep−tol region. Note that the amount of accumulation of toluene may differ when the ratio of the interface area over the bulk hep−tol volume is varied. From the density profiles, the surface excess of toluene was estimated to be $3.68 \pm 0.11 \times 10^{-6}$ mol/m^2 by taking the average for 3.0−5.0 ns, which is in fairly good accordance with the one calculated by Gibbs adsorption equation $\sim 2.93 \times 10^{-6}$ mol/m^2 (see the Supporting Information for computational details). The calculated IFT for the hep−tol−water system is 42.27 mN/m, lower than the algebraically averaged value (44.82 mN/m) for the heptane−water (51.96 mN/m) and the toluene−water (37.69 mN/m) systems. The lowered IFT should thus result from the accumulation of toluene at the hep−tol−water interface. Interestingly, the measured value is reported to be around 40 mN/m,[29,31] which is somewhat lower than our calculated value. This disparity is not a failure of the force field we used but rather may be direct proof that the interfacial tension of the hep−tol−water interface is a function of the ratio between the volume and the interface area of the heptane−toluene phase. Recall that the ratio between the volume and interface area in our MD calculation (∼6.4 nm) is extremely small compared with that of the experiment (∼167 000 nm).[29] To confirm this, we performed two additional simulations, one at a lower volume−area ratio of 3.3 nm and the other at a higher ratio of 9.5 nm. The IFTs were increased to 43.64 or reduced to 42.08 mN/m, respectively. In other words, the IFT of this system is not an intrinsic property of the interface but shows clear evidence of surfactant-like behavior[29] (of toluene). In summary, the results of the hep−tol−water system

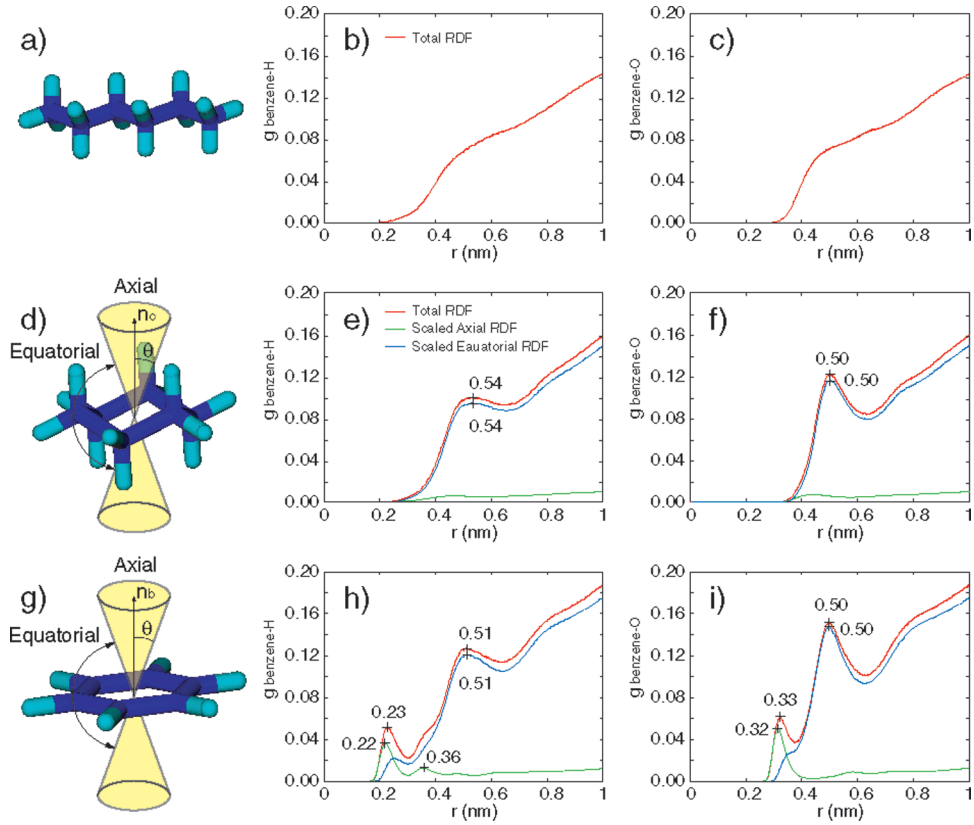

Figure 3. Total (red), axial (green), and equatorial (blue) radial distribution functions between the center of hexane (b and c), cyclohexane (e and f), benzene (h and i), and hydrogen (middle panels) or oxygen (right panels) in water molecules in each hydrocarbon−water interfacial system. Note: only those of benzene with water present two apparent peaks. The molecular frames of hexane, cyclohexane, and benzene are shown in the left panels for comparison. In particular, a schematic of the definition of the axial and equatorial RDFs for benzene and cyclohexane is shown, together with those of the molecular frame. The axial and equatorial RDFs are related by following equation: $g_{\text{normal}}(r) = g_{\text{axial}}(r)(1 - \cos\phi) + g_{\text{equatorial}}(r)\cos\phi$, where ϕ (20°) is the dividing angle between the axial and equatorial regions. The RDFs for the axial and equatorial regions were scaled by $(1 - \cos 20°)$ and $\cos 20°$, respectively. The first peaks of total RDFs of benzene and water are mainly from the axial region (see text for further details).

support our hypothesis that the accumulation is due to the mixing effects of the aromatics and the other hydrocarbons, namely, the IFT difference is the "driving force" of accumulation of aromatics.

The "Weak Hydrogen Bonding" between Aromatics and Water. In the following, we show that the reason the aromatics−water interface has a lower IFT is that there is attractive "weak hydrogen bonding" between aromatic molecules and water molecules.[34−38] Parts b, c, e, f, h, and i of Figure 3 show the radial distribution functions (RDFs) between the center of hexane, cyclohexane, benzene, and the hydrogen or oxygen atoms in water molecules in each hydrocarbon−water interface system. In sharp contrast to the hexane−water and the cyclohexane−water interface systems (which have only one peak at around $r = 0.5$ nm, Figure 3, parts b, c, e, and f), the total RDF, g_{total}, in the benzene−water interface system has two peaks (Figure 3, parts h and i). To explain why these two peaks appear, the total RDFs in the cyclohexane−water and benzene−water interface system were divided into two regions: the axial and equatorial regions, $g_{\text{axial}}(r)$ and $g_{\text{equatorial}}(r)$ (as shown in Figure 3, parts d and g), respectively. The RDFs are defined by $g_{\text{total}}(r) = g_{\text{axial}}(r)(1 - \cos\phi) + g_{\text{equatorial}}(r)\cos\phi$, where ϕ is the dividing angle between the axial and equatorial regions. In the present case, ϕ was set to 20°. The first peaks of each g_{total} in the benzene−water interface system are mainly contributed by $g_{\text{axial}}(r)$ (Figure 3, parts h and i). In particular, the $g_{\text{benzene−H}}$ and $g_{\text{benzene−O}}$ show maximum values at $z = 0.23$ and 0.33 nm, respectively. The difference is exactly 1 Å, a value close to the OH bond length in the water molecule. We therefore, confirm the picture of "weak hydrogen bonding", i.e., the nearest water molecule in the axial region tends to point its proton toward the benzene ring. To investigate and compare the details of this local structure, one additional MD calculation of the solution system (one benzene molecule and 2176 water molecules) was performed at 298 K and 0.1 MPa. Figure 4 shows the angular-dependent RDFs for this "artificial" solution and the benzene−water interface system. In both systems, $g_{\text{benzene−H}}$ and $g_{\text{benzene−O}}$ show maximum values at $z = 0.21$ and 0.31 nm, respectively, at an angle of less than 20°. The nearest water molecule to benzene locates well in the normal direction to the benzene ring, and its hydrogen is oriented toward the center of benzene. This situation provides a strong basis for the dividing angle (20°) used for Figure 3. In other words, the benzene molecules near the interface display "weak hydrogen bonding" between the aromatic rings and the proton of the water molecules in the interface system. Although we have shown here only the analysis

(34) Suzuki, S.; Green, P. G.; Bumgarner, R. E.; Dasgupta, S.; Goddard, W. A., III; Blake, G. A. *Science* **1992**, *257*, 942–945.
(35) Raschke, T. M.; Levitt, M. *Proc. Natl. Acad. Sci. U.S.A.* **2005**, *102*, 6777–6782.
(36) Allesch, M.; Lightstone, F. C.; Schwegler, E.; Galli, G. *J. Chem. Phys.* **2008**, *128*, 014501.
(37) Schravendijk, P.; van der Vegt, N. F. A. *J. Chem. Theory Comput.* **2005**, *1*, 643–652.
(38) Graziano, G.; Lee, B. *J. Phys. Chem. B* **2001**, *105*, 10367–10372.

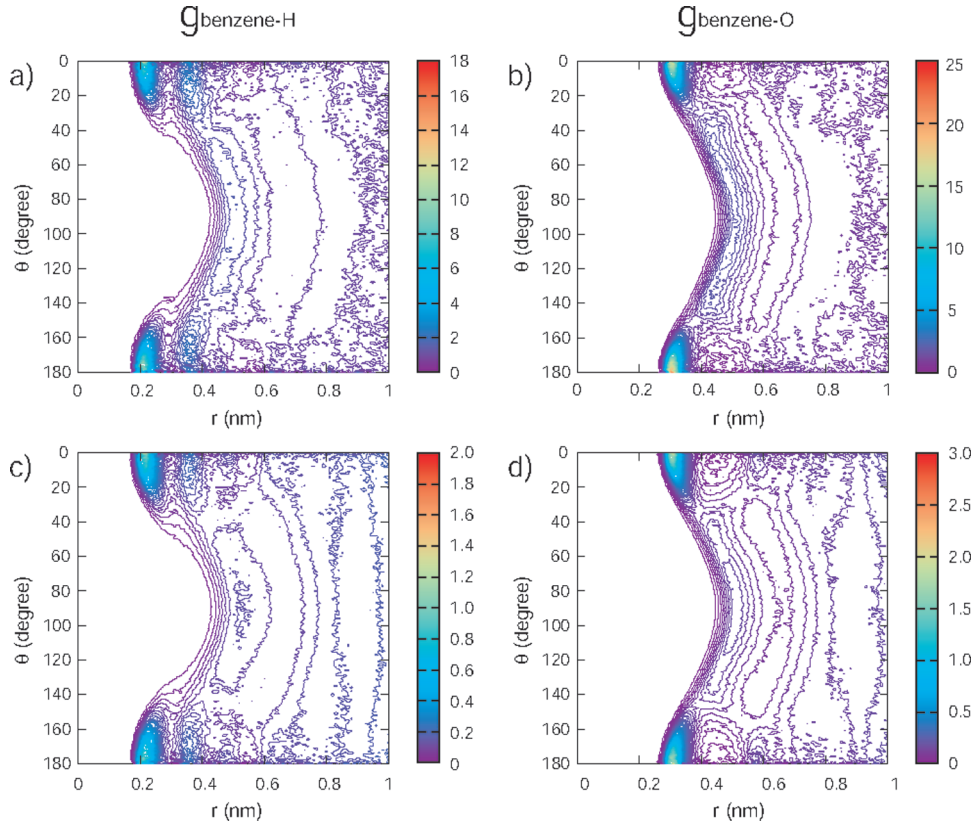

Figure 4. Angle-dependent RDFs from the center of benzene and the hydrogen or oxygen atoms in water molecules. The base direction was set normal to the benzene ring plane: (a and b) the solution system; (c and d) the benzene−water interfacial system.

of the pure benzene−water interface, a similar finding holds for the toluene−water interface. The attractive nature of this "weak hydrogen bonding" is the reason aromatics have a lower interfacial tension with water than the other hydrocarbons.

Charge Dependence of the Benzene Model: A Further Evidence of the Weak Hydrogen Bonding. To further confirm the presence of weak hydrogen bonding, the charge dependence was investigated. Although the default charge value for hydrogen atoms in a benzene molecule in the CHARMM27 force field is 0.115, values of 0.120, 0.125, and 0.130 were also investigated (the values for carbon atoms were the negative of each hydrogen charge value) at 298 K and 0.1 MPa. The IFTs showed lower values when the model had a higher charge set. Interestingly, the model with a proper charge of ∼0.130, which provides the experimental interfacial tension, reproduced the density of the pure benzene phase. Therefore, a charge set of 0.130 was used for the benzene model in the light-oil model as well as the pure benzene−water interface, as shown in Figures 2−4. Aromatic molecules interact with each other through so-called "$\pi-\pi$ stacking" in which the π systems form two parallel rings overlapping in a "face-to-face" orientation. They also interact in an "edge-to-face" orientation[39] where the slight positive charges of substituents on the ring atoms of one molecule are attracted to the slight negative charge of the aromatic system on another molecule. The configuration with a higher "edge-to-face" orientation is typically higher (as manifested by high-pressure polymorphs of benzene[39]) and can explain the observed behavior that the bulk densities show higher values with higher absolute value of electric charges. Although Lorentzian−Bertzian rules were used throughout our study, we also tested different Lennard-Jones potential parameters, as van Buuren et al. had done for the decane−water interface.[15] It is concluded that the interfacial tension is mainly dominated by a Coulomb interaction via weak hydrogen bonding, which differs from previous findings based on the analysis of the hydration Gibbs free energy.[38]

Conclusions

Finally, it is remarkable that the accumulation of aromatics is fundamentally different from the layering of alkanols at the oil−water interface and those observed in case of surfactants,[18,33] which are well-known amphiphilic behaviors. Such accumulation (or the weak hydrogen bonding) might be detected by vibrational sum frequency spectroscopy,[7,8] novel near-field or fourth-order coherent Raman spectroscopy,[9,10] or spatially resolved NMR spectroscopy.[11] In particular, the NMR signals of protons in the plane of an aromatic ring are shifted substantially from those on nonaromatic hydrocarbons. This is an important method to detect the accumulation of aromatics at the oil−water interface. Although the amount of the aromatics accumulation decreases under high-temperature and high-pressure conditions, the phenomenon would generally occur under reservoir conditions. These aromatics-rich layer formations may be a critical factor in determining the interfacial behaviors in EOR technology. It might be straightforward to generalize our findings to the notion that interfacial tension difference is a driving force for the probable accumulation of materials at other mixture interfaces, which are ubiquitous and important to many natural and technological processes.

(39) Raiteri, P.; Martonak, R.; Parrinello, M. *Angew. Chem., Int. Ed.* **2005**, *44*, 3769–3773.

Acknowledgment. The authors thank JOGMEC and JAPEX for financial support and valuable discussion with Y. Fukunaka. C.R.M. acknowledges CNPq, FAPESP, and UFABC for funding. M.K. is grateful for a Japan Society of the Promotion of Science Research Fellowship through KAKENHI 226752. The snapshot shown in our paper was prepared by Visual Molecular Dynamics (VMD) software for visualizing molecular dynamic trajectories.

Supporting Information Available: Additional discussion and figures of the computational systems and methods and the interfacial tension of the heptane−toluene−water system. This material is available free of charge via the Internet at http://pubs.acs.org.

JA107519D